

Materials Horizons

Accepted Manuscript

This article can be cited before page numbers have been issued, to do this please use: B. T. Wilcox, E. T. Williams and M. D. Bartlett, *Mater. Horiz.*, 2025, DOI: 10.1039/D5MH00911A.



This is an Accepted Manuscript, which has been through the Royal Society of Chemistry peer review process and has been accepted for publication.

Accepted Manuscripts are published online shortly after acceptance, before technical editing, formatting and proof reading. Using this free service, authors can make their results available to the community, in citable form, before we publish the edited article. We will replace this Accepted Manuscript with the edited and formatted Advance Article as soon as it is available.

You can find more information about Accepted Manuscripts in the [Information for Authors](#).

Please note that technical editing may introduce minor changes to the text and/or graphics, which may alter content. The journal's standard [Terms & Conditions](#) and the [Ethical guidelines](#) still apply. In no event shall the Royal Society of Chemistry be held responsible for any errors or omissions in this Accepted Manuscript or any consequences arising from the use of any information it contains.

New Concepts

We introduce a new approach for creating textile-integrated, multilayer liquid metal (LM) soft circuits that combines high flexibility with advanced electrical functionality and environmental resilience. Integrating multilayer architectures and rigid components into wearable electronic textiles is challenging, and our method enables robust vertical interconnects through *vias*, strong interlayer adhesion (up to 11,000 J m⁻²) through synergistic soft welding techniques, and compatibility with surface-mounted components within a fully stretchable, textile-conformable platform. Furthermore, new mechanistic guidance is provided for designing interlayer adhesion of wearable multilayer circuits, for the structure–mechanics–functionality relationship between textile, elastomer and liquid metal, especially regarding electromechanical properties of stretchable liquid metal conductors, and for the performance of such soft circuits in aqueous environments. The utility of these wearable electronics is demonstrated through several different devices including a wearable multi-camera system that delivers a simulated bird’s-eye view, offering users an expanded, immersive awareness of their surroundings. This strategy advances the field by bridging soft electronics and textile-based systems, offering a robust and adaptable foundation for next-generation wearable devices.



Textile-integrated multilayer liquid metal soft circuits for multienvironment wearable electronics

Brittan T. Wilcox,^{1†} Ella T. Williams,^{1†} and Michael D. Bartlett^{1,2*}

¹Mechanical Engineering, Soft Materials and Structures Lab, Virginia Tech, Blacksburg, VA 24061, USA.

²Macromolecules Innovation Institute, Virginia Tech, Blacksburg, VA 24061, USA.

[†] These authors contributed equally to this work

* To whom correspondence should be addressed: mbartlett@vt.edu

Abstract

Soft devices that are rugged yet deformable are essential for wearable technologies that perform in diverse environments. For textile-based wearable electronics, creating robust mechanical and electrical interconnections between electronic components on complex, deformable surfaces like textiles remains a central challenge. In this work, we present a scheme for the creation of textile electronics through multilayer liquid metal (LM) soft circuits, including robust integration with textiles and water resistance. The fabrication method enables multilayer construction with vertical interconnect access or *vias*, as well as the integration of rigid electronic components, to enable advanced electrical functionality while maintaining flexibility and stretchability. We achieve robust interlayer adhesion (up to 11,000 J m⁻²) within the soft circuits by combining multiple soft welding processes. Furthermore, the influence of textile integration on electromechanical performance is determined, providing mechanistic guidance to enable textile-integrated LM soft circuits that stretch to 300% strain with resilience against environmental damage, including water resistance. These textile-based soft circuits enable sensing and data transfer, which we show through several examples including a distributed wearable camera system. This process is adaptable to a wide variety of circuit designs and layouts, providing a path forward for robust, textile integrated electronics.



Introduction

Creating robust interconnections between multiple electronic components across complex surfaces like textiles is a key challenge in developing advanced wearable electronics and sensor networks. Previous schemes to integrate conductive circuit materials with textiles have included encapsulating rigid printed circuit boards (PCB) on textiles with hot melt resins,¹ conductive threads woven into textiles,^{2–5} mask-printing directly onto textiles,⁶ iron-on conductive traces,^{7,8} and copper lithography encapsulated in elastomer-embedded textiles.⁹ Textile-integrated multilayer soft circuits offer a promising route to enhance wearable electronics by providing greater interconnect flexibility and mechanical conformability. Beyond flexibility, ensuring reliable operation in challenging environments is essential for the development of robust, next-generation wearables. Soft circuits are well suited to meet these demands, as they combine environmental and damage resilience with the ability to stretch and conform to complex, dynamic surfaces.

Emergent materials such as liquid metals (LM) have enabled soft circuits with new properties including extensibility, conformability, and self-healing,^{10–16} and these materials have been used in different types of soft electronics.^{17–26} Recently, electronic functions with increasing complexity have been enabled through new fabrication techniques that allow for multilayer LM soft circuits. The inclusion of vertical interconnect access (*vias*), which provide electrical connections between separate layers of a circuit, allows for greater circuit design complexity.²⁷ While rigid PCBs typically use drilled holes for *vias*, soft circuits have found alternative methods by using laser ablation,^{28–31} lift-off patterning,³² or selective stratification of LM droplets in a composite.³³ The integration of LM soft circuits into textiles has also provided a platform for wearable electronics,^{14,34–38} bringing LM soft circuits further into the forefront of next-generation devices. However, a comprehensive understanding of textile integration—including interlayer adhesion, the influence of textile substrates on electromechanical performance, and device durability in challenging environments—remains



incomplete, yet is essential for advancing the field.

Creating wearables that withstand both user interaction and environmental stresses is essential for expanding their functionality and reliability in real-world applications.^{39–43} For example, integration of water-resistant, soft, and stretchable circuits into underwater suits could enable new functionalities and ergonomic designs for underwater wearable electronics.^{36,44–48} This is especially compelling when multilayer circuit architectures, enabled by *vias*, can be combined with rigid electronic components to form hybrid systems that maintain flexibility while enhancing capability. Despite their promise, the performance of LM soft circuits under harsh conditions, particularly full water submersion, remains underexplored. However, such conditions present a valuable opportunity, as soft circuits offer inherent advantages for underwater use. Unlike rigid systems that require bulky pressure vessels, some soft electronics have operated directly in high-pressure environments, offering increased functionality.^{49,50} LM-based composites are promising in this context, having demonstrated resistance against degradation in aqueous environments,⁵¹ as well as successful implementation in recyclable underwater LM circuits⁵² and underwater sensing devices.⁴⁵ Taken together, these studies highlight the potential of LM soft circuits as robust, multilayered components for next-generation wearables, combining stretchability, environmental resilience, and advanced sensing.

Here, we advance textile-based wearable electronics by developing elastomer-encapsulated, multilayer circuits that integrate both liquid metal interconnects and rigid components into textile substrates, and we systematically characterize their electromechanical performance, interlayer adhesion, and environmental durability. The integration of circuit components with textiles through soft, extensible circuits allows many electronic and sensing components to interconnect while remaining conformable to serve as wearable electronics. This allows them to leverage advanced functionalities through traditional surface-mounted components and integrated circuits, and their multilayer construction with interlayer *vias* allows greater flexibility in circuit design. Strong interlayer adhesion, both between the elastomer



circuit layers and to the textile substrate, provides wearable electronics with a robust encapsulation and protection against challenging environments. This encapsulation allows the textile-integrated LM soft circuit to intrinsically be used underwater, even while retaining its ability to stretch and flex alongside complex electrical operation. With this, we can create wearable electronics with both stretchable wiring and rigid electronic components that are integrated with form-fitting clothing and conformable to the human body, offering a method to achieve highly interconnected networks with advanced sensing capabilities (Fig. 1a).

Results and Discussion

Fabrication of multilayer textile-integrated LM soft circuits

For the construction of wearable electronics through elastomer-integrated textiles, a matrix material is required to both serve as a medium between LM wires and textiles and as protection against the external environment. Styrene-based block copolymers, such as styrene-isoprene-styrene (SIS), styrene-isobutylene-styrene (SIBS), and styrene-ethylene/butylene-styrene (SEBS), are materials of interest for the construction of soft, extensible, and wearable circuits because of their unique elastomeric yet thermoplastic nature. In LM soft circuits, SIS has been used as both a substrate material for LM wires^{34,35,53,54} and as a matrix for conductive composites incorporating LMs.^{11–13,18,30} SIS block copolymers include segments of polystyrene and polyisoprene that form physical crosslinks which provide the material's cohesion and high elasticity, and they have found commercial use as hot melt pressure sensitive adhesives, a capability which we leverage here.^{55–58} Because the interactions between polymer chains in SIS can be disrupted by either heat or solvent, the material can be processed in a variety of ways including molding, thermal welding, and coating processes.^{21,47,59,60} Here, we use SIS as a substrate material for circuit construction as it allows for heat press processing to textiles, self-adhesion through solvent welding for the addition of further layers, and protection against damage.



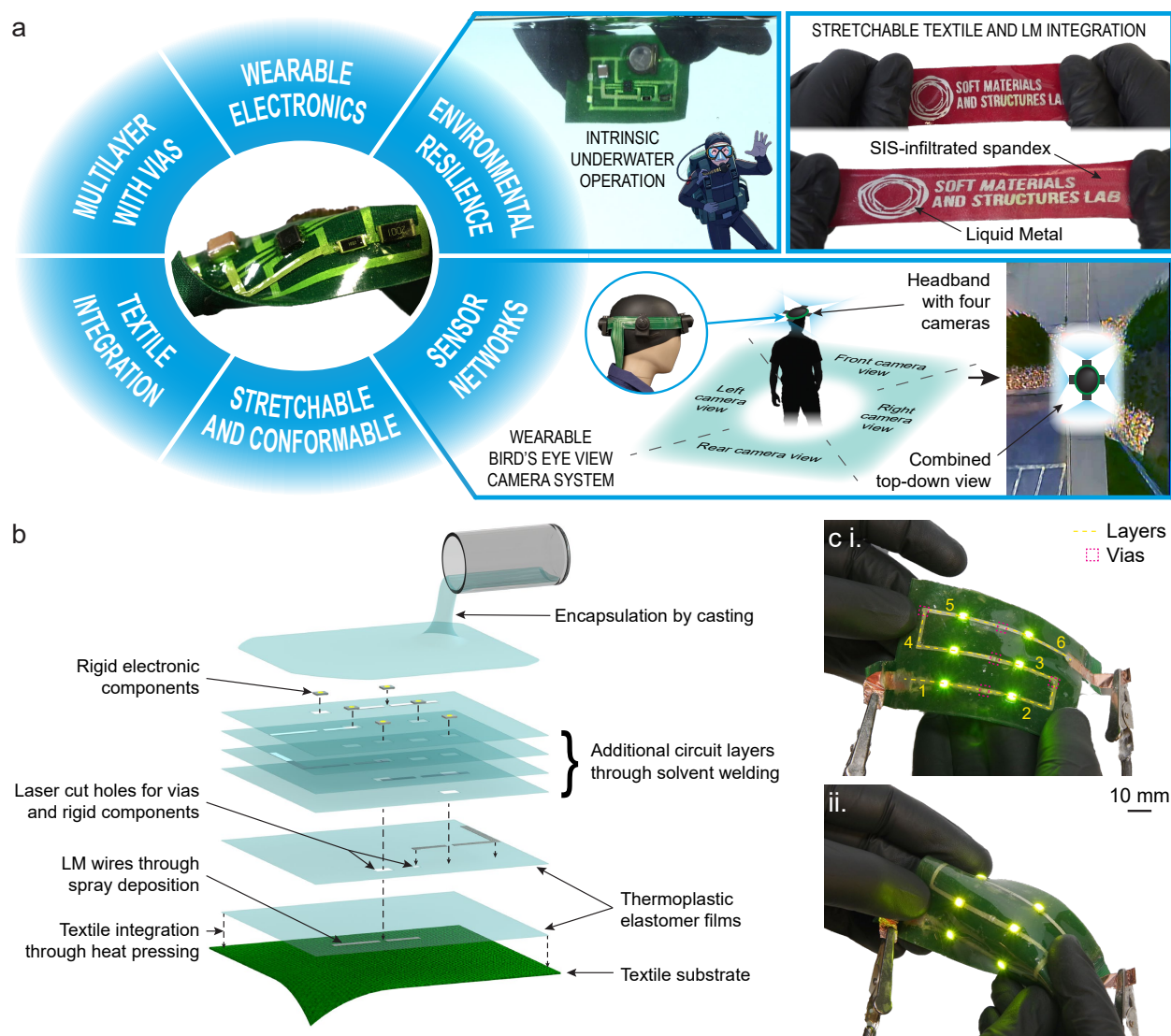


Fig. 1 Overview of textile-integrated LM soft circuits. (a) Capabilities enabled for wearable electronics, including intrinsic underwater operation (top center), stretchability (top right), and a wearable bird's eye view camera system (second row). (b) Layup of a multilayer textile-integrated LM soft circuit with rigid components embedded. (c) Images of a circuit with six LEDs in series, where each is on a different layer with a *via* between, in its normal state (i.) and folded (ii.).

The steps of the textile-integrated LM soft circuit fabrication scheme are shown through the construction of a representative six-layer circuit (Fig. 1b and S1). To begin, a sheet of SIS elastomer is bonded to a textile substrate through heat press processing. This technique achieves strong adhesion and provides a foundation upon which the circuit is constructed. LM, in this case eutectic gallium-indium (EGaIn), is deposited through spray-coating with



a stencil mask. To add additional layers, sheets of SIS are laser cut to include *via* holes and spaces for rigid components. These sheets are aligned and bonded to the circuit by solvent welding with toluene. LM for subsequent circuit layers is deposited and further SIS sheets are stacked until all layers have been completed; this process could include as many layers as are needed. Rigid electronic components are placed in the prepared spaces after all layers are deposited, and the completed circuit is encapsulated by casting further SIS over the prior layers and rigid components. A sample circuit with same design as the schematic is fabricated, in which six light emitting diodes (LEDs) are placed, each on one of six layers, with *vias* in between (Fig. 1c). This forms a series circuit of LEDs in which all successfully turn on when external power is applied. This fabrication scheme also allows for circuits to be stretchable when constructed using an extensible textile such as spandex (Fig. 1a upper right and supplementary video S1). Our approach, which enables textile integration with strong adhesion, multilayer soft circuits with *vias* that are extensible and conformable, and rigid electronic component implementation, provides a robust scheme for wearable electronics.

Adhesion of elastomer layers and textiles

Robust adhesion between elastomer films and textile substrates can be obtained by heat press processing of SIS films to a variety of textiles (Fig. 2a). Adhesive fracture energies are found through T-peel testing to be consistently greater than 1,000 J m⁻², and even exceeding 11,000 J m⁻² for a 1,000 denier polyester. These are calculated from the steady-state plateau region of the force-extension curve measured during peeling (Fig. 2a inset) using the function $G_c = 2F_c/w$, where G_c is adhesive fracture energy, F_c is the steady-state force, and w is the width of the T-peel specimen, with adjustments for extensibility of textile adherends forgone.⁶¹ Optical microscopy demonstrates that elastomer infiltrates better into noncoated textiles of both woven and knit varieties, leading to generally higher adhesion values (Fig. 2b and S2). In coated textiles such as polyester (Fig. 2b i. and ii.), the elastomer remains at the surfaces. This leads to an increased dependence on the surface



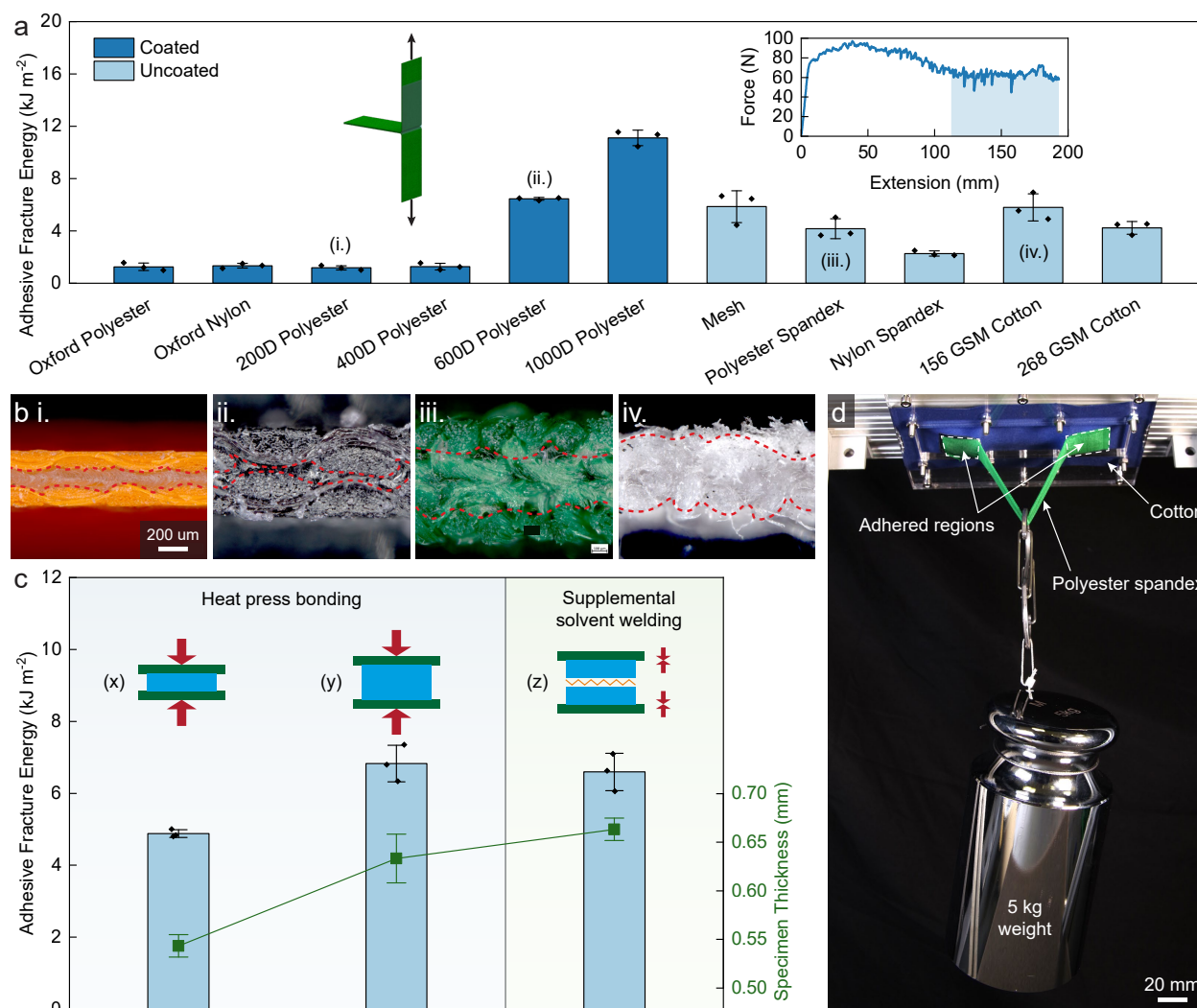


Fig. 2 Adhesion of elastomeric substrate to textiles. (a) Adhesive fracture energy for adhesion of SIS to various textile adherends. Error bars represent 1 s.d. for $n = 3$ measurements. Insets display a schematic of a T-peel specimen and an example force-extension curve on 156 GSM cotton. Adhesive fracture energy is calculated from the steady-state plateau region of the curve (highlighted). Labels i-iv correspond to the (b) micrographs of the side view of T-peel samples of (i.) 200 denier polyester, (ii.) 600 denier polyester, (iii.) polyester spandex, and (iv.) 156 GSM cotton. Red dashed lines indicate the greatest extent of elastomer impregnation. (c) Adhesive fracture energy of (x) a single layer of SIS heat pressed to textile adherends, (y) two layers of SIS heat pressed to textile adherends, and (z) two textile-integrated layers of SIS with a solvent welded interface between. Error bars represent 1 s.d. for $n = 3$ measurements. (d) A 5 kg weight hangs from an adhesive joint on an elastic textile.

topography and compatibility, whereas textiles without coatings or a less dense weave, such as polyester spandex (Fig. 2b iii.) or cotton (Fig. 2b iv.), achieve high adhesive strengths



due to a greater ability to infiltrate and interlock within the threads. Further information on the textile weaves, materials, coatings, and thread weights can be found in Table S1.

While heat press processing provides strong bonding to a textile substrate, its high process temperature and compressive stress are not conducive to the construction of additional soft circuit layers which include LM wires and rigid components. Instead, solvent welding provides a powerful technique to adhere further layers of SIS to the SIS-textile substrate. Fracture energy is therefore quantified for a textile-integrated structure that also includes solvent welding. Here, heat press bonded T-peel samples of two thicknesses, made using either one or two layers of SIS (Fig. 2c (x) and (y), respectively) are compared to a T-peel sample which includes a solvent welded interface between two layers of textile-bonded SIS (Fig. 2c (z)). The sample which includes a solvent welded interface was constructed by first heat press processing SIS to a single textile adherend, thus leaving an open surface of elastomer, then taking two of those and welding them together with toluene to form a T-peel sample. A comparative analysis of these reveals that the interlayer adhesion achieved through solvent welding between layers of SIS exhibits at least comparable strength to that of integration with textile substrates by heat press processing. Since an increase in thickness of the adhesive provides a greater volume with which to dissipate energy during fracture, the data point for solely heat press processing using two layers of SIS is provided in which the thickness is similar to the solvent welding sample; thickness values of test specimens were measured to confirm parity (Fig. 2c right y-axis). Additionally, the crack propagation during T-peel testing occurred along the elastomer-textile interface even in the test specimens with the added solvent welded interface.

To further demonstrate the high strength of our adhesion to textile substrates, a 5 kg mass is hung from a structure using this adhesion process (Fig. 2d). Here, a rigid textile is mechanically fixed to a superstructure, and an adhered strip of spandex supports the hanging weight with only two adhered regions of 25 x 25 mm each. This high strength of adhesion enables robust textile integration of our wearable circuits to prepare them for



rugged applications such as underwater use. Both the heat press processing and solvent welding techniques prevent delamination of the LM soft multilayer circuits, ensuring they both remain affixed to the textile substrate of interest and maintain their cohesion between layers.

Stiffness of multilayer textile-integrated system

This adhesion allows textiles to be integrated with SIS-based LM soft multilayer circuits which can stretch and fold while remaining operable. The extensible substrate textiles (spandex, mesh, and cotton jersey materials) serve not only to provide integration into garments, but also serve as a mechanical reinforcement for stretchable soft circuits. Knit textiles offer extensibility beyond that of their constituent fibers through a looped structure, in which gaps between fibers open.⁶² However, the exact mechanical properties of a textile-elastomer structure are influenced by complex geometry, material interfaces, and nonlinear effects.⁶³ Thus, how these nonlinear textile mechanics influence the ultimate compliance of our textile-integrated LM soft circuits needs to be investigated.

We observe that the mechanics of the textile-elastomer system under uniaxial strain vary greatly depending on the direction of loading relative to the knit pattern (Fig. 3a). The effect of integrating elastomer is different in each knit textile direction. When loaded in the wale direction (in the lengthwise direction, and parallel to the selvage edge), the stiffness is significantly increased at lower strains (Fig. 3b i.) but the structure is weakened, both in a reduction of ultimate tensile strength and strain at break. When loaded in the course direction, (in the crosswise direction) the material is much more compliant than in the wale direction and the stress-strain response is similar to that of the textile alone. The elastomer still provides an increase in stiffness at low strains (Fig. 3c i.), but this becomes negligible at higher strains. In contrast to loading in the wale direction, the elastomer acts to strengthen the material when loading in the course direction, as it is capable of withstanding greater stresses and strains when elastomer is integrated. These varying changes to the mechanical



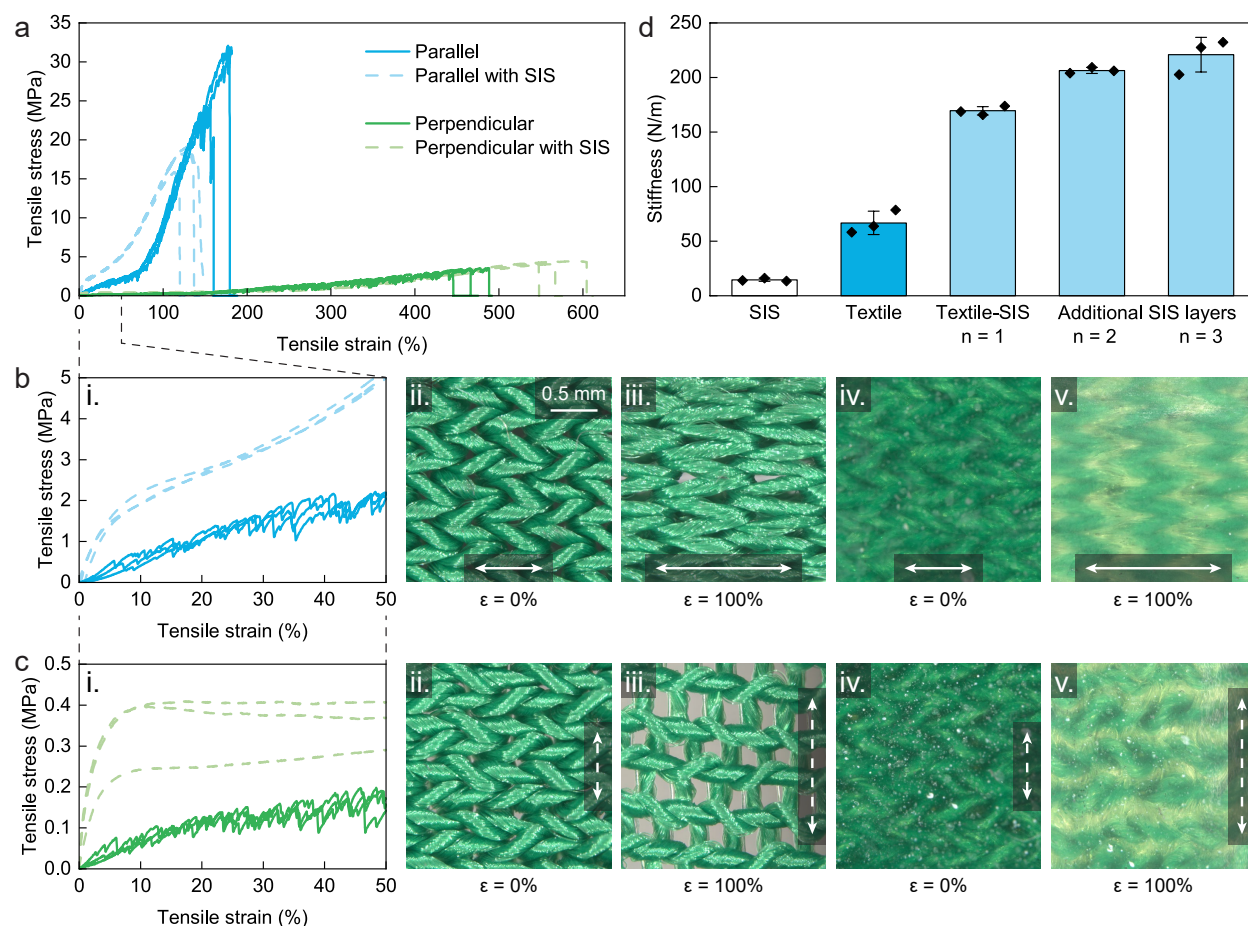


Fig. 3 Mechanical characterization of textile-elastomer substrate. (a) Stress-strain curves for polyester spandex textiles under uniaxial tension in the wale and course directions, both with and without SIS adhered. (b) (i.) Stress-strain curves up to 50% strain for loading in the wale direction. Microscope images of wale-strained textile at (ii.) $\epsilon = 0\%$ and (iii.) 100% and textile-elastomer substrate at (iv.) $\epsilon = 0\%$ and (v.) 100%. (c) (i.) Stress-strain curves up to 50% strain for loading in the course direction. Microscope images of course-strained textile at (ii.) $\epsilon = 0\%$ and (iii.) 100% and textile-elastomer substrate at (iv.) $\epsilon = 0\%$ and (v.) 100%. (d) Stiffness (taken at 50% strain) for SIS, polyester spandex textiles strained in the wale direction as is and with added layers of SIS. Error bars represent 1 s.d. for $n = 3$ measurements.

performance of a textile-elastomer system compared to either of its constituents suggests that in knit textiles, the manner in which elastomer infiltrates the textile structure results in a composite-like response rather than a layered response (Fig 3b,c ii-v.).^{63,64} This further varies significantly across different extensible textile materials integrated with elastomer (Fig S3). Because many of the textile structures exhibit non-homogeneous strain distributions



by opening up gaps between threads when stretched⁶² (Fig. S4), the mechanics could be altered through the infiltration of elastomer between the textile fibers.

With this fabrication method for multilayer textile-integrated LM soft circuits, each added layer expands the circuit's functional complexity through additional routing, sensing, or interfacing capabilities, while only reducing deformability of the device to a lesser extent through slight increases in overall thickness. To understand how additional layers impact compliance, we measure the stiffness at 50% strain in the wale direction, representative of upper-bound deformations in typical wearable use cases, for devices with varying numbers of elastomer circuit layers (Fig. 3d). While the first elastomer layer introduces the greatest increase in stiffness through embedding into the textile, subsequent layers contribute more modestly, indicating that the added layers behave mechanically as discrete additions rather than forming a fully bonded composite structure. This layered architecture preserves overall compliance while enabling increased functional density. This structure-mechanics-functionality relationship allows for the integration of complex soft circuits with multilayer interconnects and hybrid components with dramatic deformability, enabling greater functionality without compromising ergonomics.

Electromechanical properties of textile-integrated LM soft circuits

To evaluate the applicability of textile-integrated LM soft circuits in highly stretchable textiles such as spandex, electromechanical characterization was performed. In these tests, a single representative wire of the LM soft circuit, encapsulated between elastomer layers formed into tensile dogbones, is extended under tensile loading while the resistance is measured with a four-point probe. Samples for these tests include both elastomer and LM only and ones integrated with a textile layer (polyester spandex). The LM-elastomer system (SIS-LM wire) is shown to stretch to greater than 2000% strain at fracture under tensile loading, while the addition of a bonded stretchable textile layer (SIS-LM wire on spandex) reduces this to about 600% strain (Fig. 4a i. and S5).



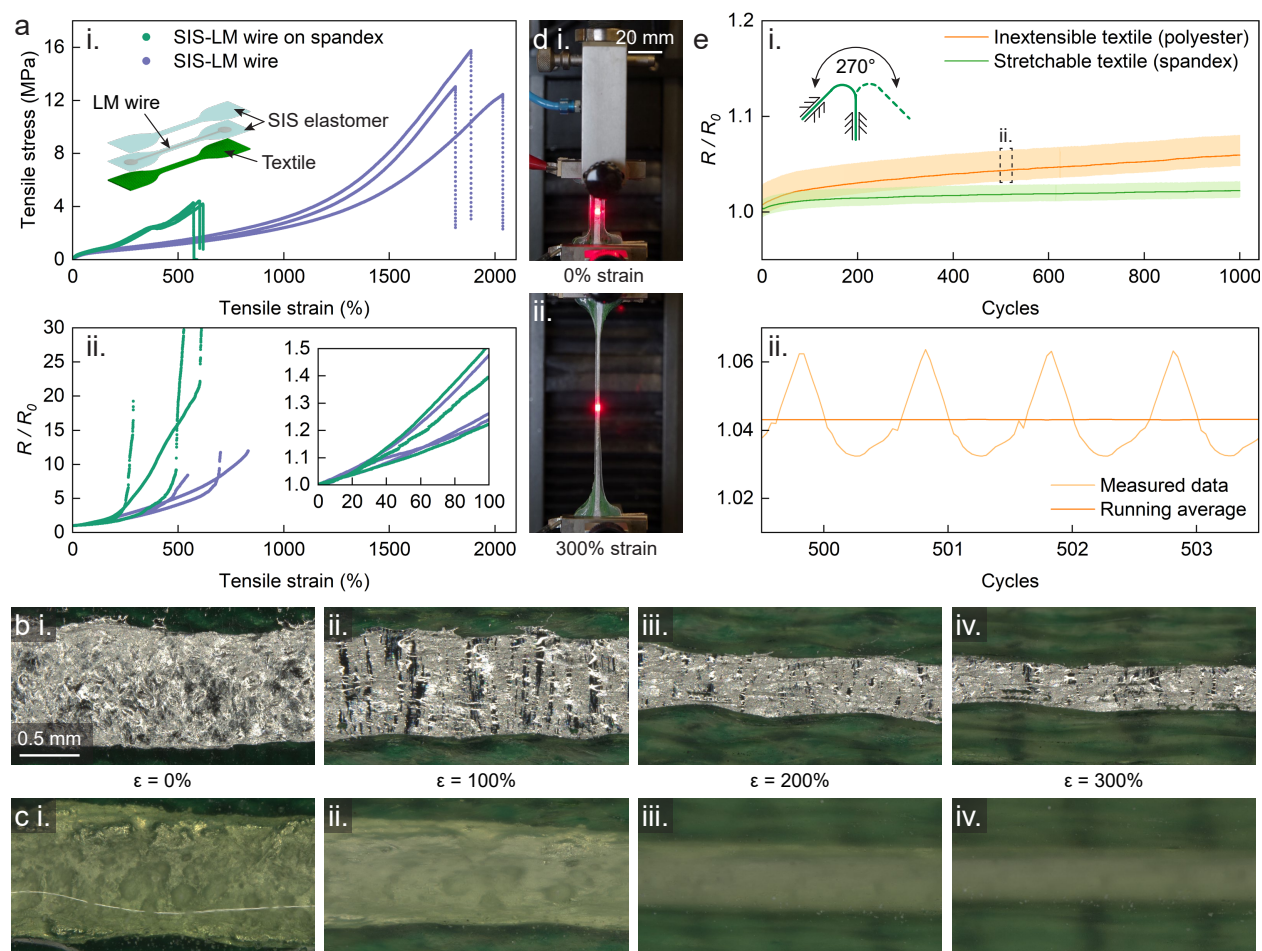


Fig. 4 Electromechanical characterization of textile-integrated LM soft circuits. (a) (i.) Tensile mechanical response of LM wires in the soft circuits, both with and without bonded textile. Inset depicts sample layout. (ii.) Normalized resistance for same specimens as in (i.). Inset shows initial range from 0 to 100% strain during which minimal change occurs. (b) Demonstration of a textile-integrated LM soft circuit with a rigid LED structure on a polyester spandex substrate strained to 300% of original length. (c) Microscope images of a LM wire on elastomer-integrated textile at (i.) $\epsilon = 0\%$, (ii.) $\epsilon = 100\%$, (iii.) $\epsilon = 200\%$, and (iv.) $\epsilon = 300\%$. (d) Microscope images of a LM wire on elastomer-integrated textile and encapsulated by further elastomer at (i.) $\epsilon = 0\%$, (ii.) $\epsilon = 100\%$, (iii.) $\epsilon = 200\%$, and (iv.) $\epsilon = 300\%$. (e) (i) Normalized resistance during 1000 cycles of folding, with inset displaying test setup, and (ii) measured data and running average for 3 representative cycles.

Normalized resistance (R/R_0), the electrical resistance (R) relative to the initial undeformed state (R_0), is measured over the same tensile extension (Fig. 4a ii.). Here, the specimens bonded to textile substrates show electrical failure of the LM wire at lower strains than material fracture. For all cases, system conductivity is lost prior to specimen fracture



due to discontinuities developing in the LM wire that prevent a continuous conductive pathway. One textile-bonded test specimen retains some conductivity up until mechanical failure at about 600% strain, but prior to that showed a sharp increase in electrical resistance above 250% strain. Both samples with and without textile layers show similar electromechanical trends at low strain ($\sim 100\%$), indicating that the integration of a textile layer for LM soft circuits does not degrade conductivity at the strains expected in wearable electronics. This suggests that the relationship between the layup of the structure and the electromechanics of a LM wire does not have an influence at low strains. At higher strains, the specimens with bonded spandex begin to lose conductivity prior to specimens of just elastomer and LM. This may be due to highly localized stress concentrations resulting from the nonlinear deformation response of stretchable knit textiles and their interaction with the elastomer integrated between their fibers. Even with the addition of rigid components such as LEDs, the textile-integrated LM soft circuit retains functionality at strains of up to 300% (Fig. 4b and supplementary video S1).

To further investigate the mechanics driving electrical continuity disruption, we examine LM wires subject to uniaxial strain under a microscope. For LM wires without encapsulation, we observe the emergence of gaps normal to the direction of the applied tension (Fig. 4c). These gaps provide an explanation for why resistance sharply increases at different strains for each specimen in the electromechanical data previously measured (Fig. 4a ii.); since a disruption of electrical continuity could be caused by propagation of only a single gap across the entire width of the LM wire, the presence of many gaps in even only 1 mm of LM wire leads to this failure being highly driven by probability. When encapsulated by elastomer, it appears that these gaps may not form as readily (Fig. 4d). Additionally, the stretchable knit textiles exhibit significant out-of-plane bending (i.e., curling) at high strains, which may also contribute to the electromechanical performance.

Textile-integrated specimens are also subjected to a cyclic folding test (Fig. 4e and supplementary video S2) and a cyclic tensile test (Fig. S6), and show stable behavior. This



measures the resilience of soft circuits subjected to the manipulation they would see in use, as this response can be dependent on the materials present.^{65–71} For textile-integrated LM soft circuits, resistance is shown to have minimal change over 1000 cycles of folding (Fig. 4e i.). Both stretchable and inextensible textiles were investigated across 5 test specimens each (Fig. S7), with a single, median representative being presented. The darker line is a running average representing the overall trend in resistance, while the shaded region represents the resistance change during each fold (see also Fig. 4e ii.). The inextensible textile backings exhibited a slightly greater tendency to cause an increase in resistance over time. This further shows that the integration of elastomer and textile enables LM wires to retain their electrical properties and functionality during use. This enables a textile-integrated LM soft circuit system that is robust against manipulation such as stretching and folding, which provides desirable properties for use in wearable electronics.

Application of textile-bonded LM soft circuits to underwater environments

By fully encapsulating the soft circuit, these textile-integrated wearable electronics are resistant to aqueous environments. We demonstrate this by immersing circuits in water, during which the circuits retain functionality. This includes a tensile test after water immersion for 24 hours, showing no change in the electromechanical nor mechanical response of the LM wire (Fig. S8), as well as a test of ingress protection against water based on the IPX7 rating in the IEC 60529 standard (Fig. 5a and Supplementary video S3), which demands submersion to a depth of 1 meter for 30 minutes to evaluate water resistance. We immerse a fully encapsulated textile-integrated LM soft circuit consisting of a battery, resistor, and LED to this depth and record it with a camera and timer. Continual operation of the LED is shown during the entire duration, demonstrating successful protection against water damage under the same conditions as a standardized rating for consumer electronic devices. Furthermore, we show stable functionality of textile-integrated and encapsulated LM wires immersed in



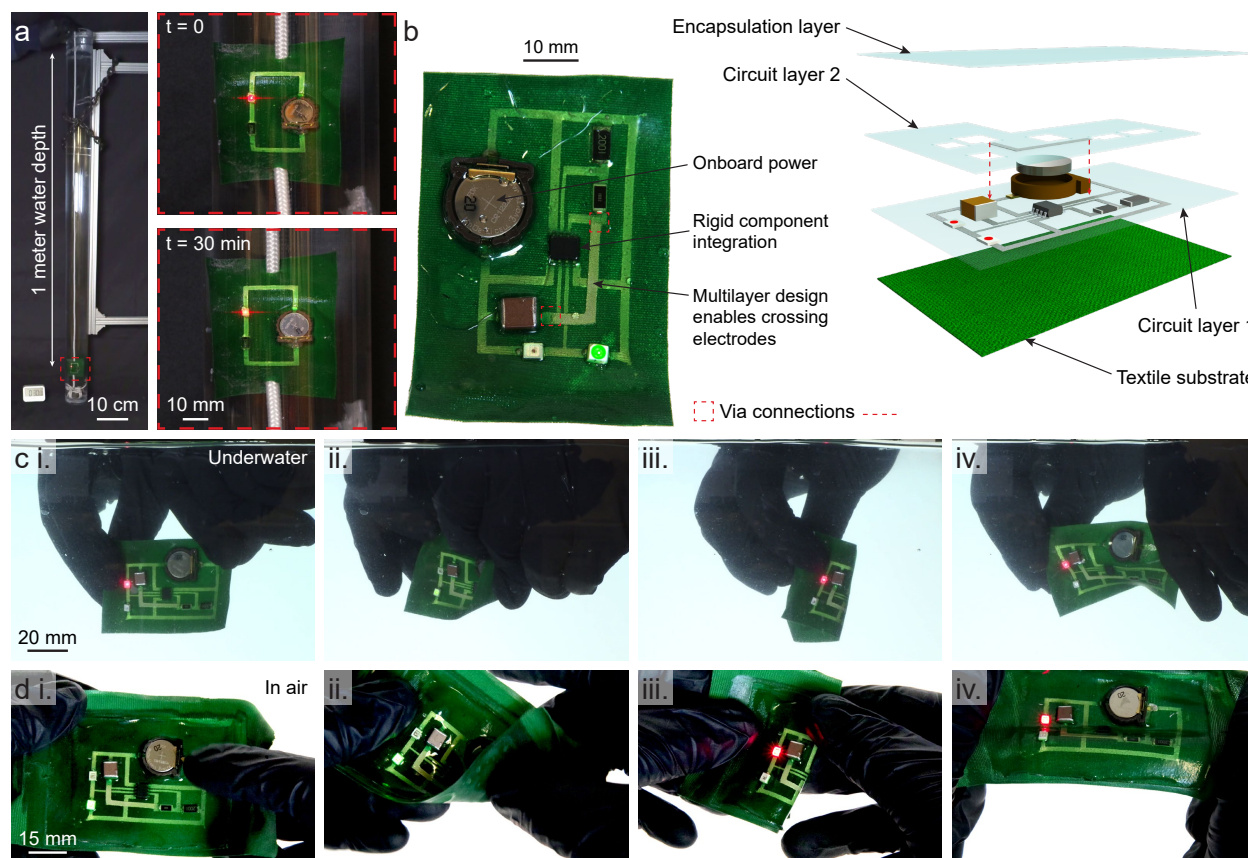


Fig. 5 Underwater demonstrations of flexible and stretchable textile-integrated LM soft circuits. (a) IPX7 water immersion test of a representative circuit, which is still functioning after 30 minutes at a depth of 1 meter. (b) Sample two-layer circuit in which two LEDs blink in alternate using a 555 timer chip, and (c) its operation in underwater and (d) dry environments, including (ii., iii.) folding and (iv.) stretching.

hot and cold environments, including 0°C freezing water, 50°C hot water, and 80°C air, with only minimal temperature dependence in the resistivity of the LM wire and a return to its original properties after temperature exposures (Fig. S9).

The integration of more complex circuits is shown through the construction of an alternating flash LED circuit utilizing an IC, onboard power, and multiple rigid electronic components (Fig. 5b). This circuit includes an 8-pin timer IC, a coin cell battery, and resistors and capacitors which make a pair of red and green LEDs flash in an alternating pattern. Due to the required connections, this circuit would not be possible in a single-layer configuration using this specific model of timer IC, and multiple *vias* are used to allow LM



soft conductive traces to cross over each other in a multilayer design. The elastomer encapsulation enables this circuit to operate when immersed in water, including still being foldable and stretchable (Fig. 5c,d and supplementary video S4). This inherent water resistance is enabled by the elastomer encapsulation, which neither absorbs water (Fig. S10) nor permits the transmission of water vapor (Fig. S11). The capability of these textile-integrated LM soft circuits to survive submersion in water without additional protective structures or potting compounds shows potential for their use in more varied applications, such as wearable components on dive suits or as part of soft underwater robots. Furthermore, by removing rigid-rigid interfaces, soft circuit structures such as these show future possibilities for hydrostatic pressure resilient electronic systems.⁷² Thus, in addition to multilayer construction and textile integration, this fabrication method also provides multiple benefits through inherent fortification against aqueous environments and hydrostatic pressure for next-generation underwater electronics.

Application of textile-bonded LM soft circuits to wearable sensing

In addition to underwater applications, we also demonstrate the ability of these textile-integrated LM soft circuits to facilitate advanced wearable electronics capable of functions such as environmental sensing. Using a multilayer LM soft circuit bonded to an extensible textile, we create a wearable device that provides a user with a complete overhead bird's eye view of their surroundings in all directions. This device is designed as a conformable and unobtrusive headband-like garment which serves as a mounting point for four orthogonally-facing cameras (Fig. 6a). Each camera requires a devoted power, ground, and analog signal wire connected to a processor, which warps and stitches the video feeds into the overhead view; this is provided through a circuit containing two layers with six traces of LM wiring each for a total of 12 traces, with a sum total of 4.2 meters of LM wiring throughout (Fig. 6b). The LM wiring is capable of transmitting 25 frames per second (through a phase alternating line protocol) from four cameras to the central processor, demonstrating the capability of



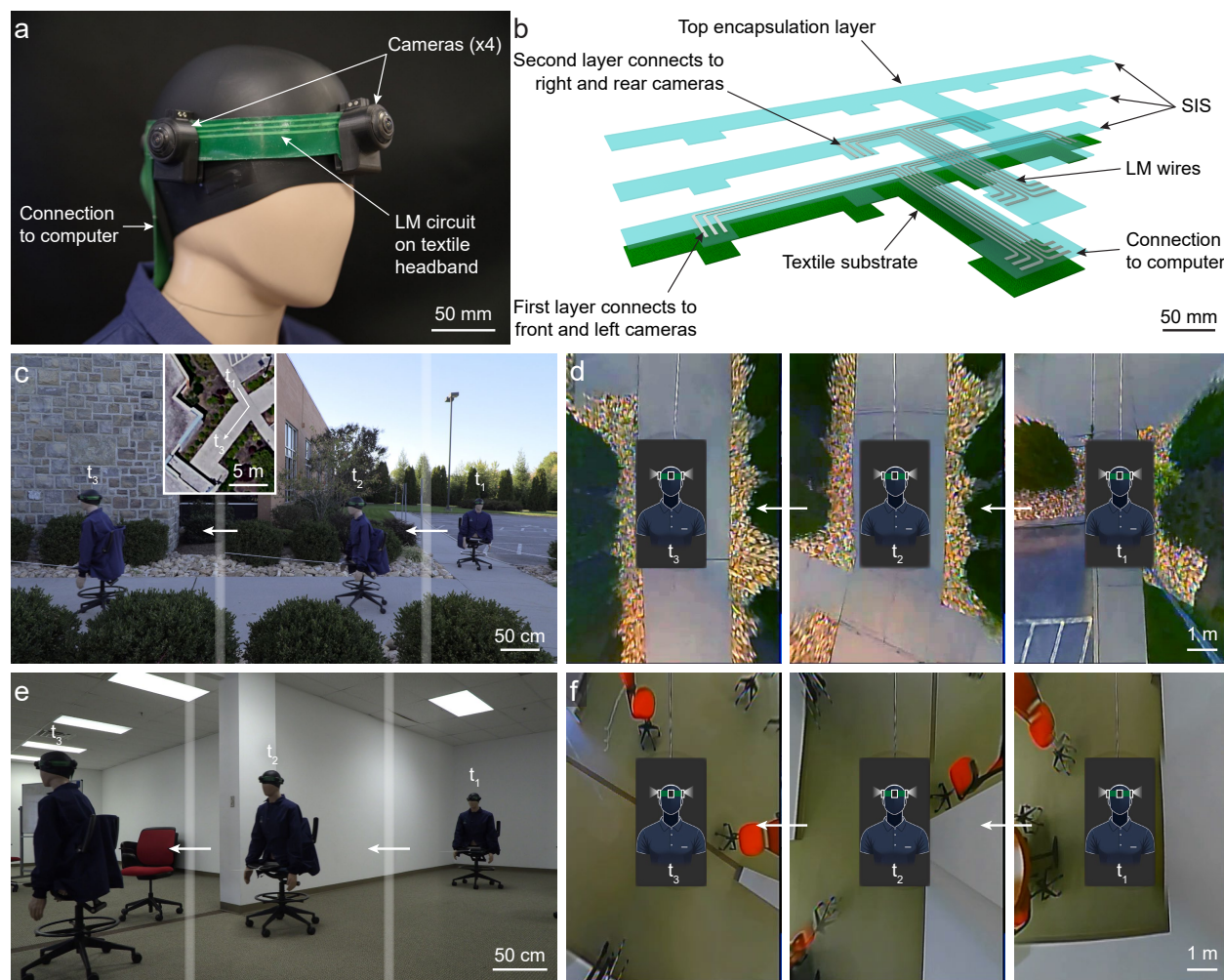


Fig. 6 Applications of textile-integrated LM soft circuits to wearable sensing. (a) Image of headband with four cameras placed on a mannequin. (b) Exploded-view schematic of wearable headband circuit. (c) Demonstration of the four-camera headband system being moved through an outdoor environment while (d) recording a stitched overhead view, shown at three different times, t_1 , t_2 , and t_3 . Inset image in (c) shows satellite view of area (Maps data: Google ©2024). (e) Demonstration of the four-camera headband system being moved through an indoor office space environment while (f) recording a stitched overhead view, shown at three different times, t_4 , t_5 , and t_6 .

the LM wires to carry large amounts of data in real time over extended lengths.

The camera system is trialed in outdoor (Fig. 6c,d) and indoor (Fig 6e,f) environments. In both open and constrained environments, the wearable bird's eye view system is capable of collecting and recording not only the four independent camera views, but also the stitched overhead view (supplementary video S5). Additionally, the stitched overhead view is pro-



vided in real-time to an external screen. This wearable device expands beyond current body camera technology in that it provides information in real time for situational awareness and can record 360° context for body cameras used for incident recording. The networking of multiple body cameras together using LM wires to transmit power and data enables new functions like the overhead bird's eye view in wearable sensing, but also shows potential for multiple wearable sensors to form sensor networks, such as for health monitoring or situational awareness. This type of sensor fusion can greatly benefit from the ability to create advanced, multilayer circuits that are integrated with textiles, and this textile-integrated process provides a foundation for the addition of advanced sensor networks to garments.

Conclusions

We create LM soft circuits which achieve robust adhesion to textiles, are foldable and stretchable, can use multilayer designs with *vias* as well as many rigid components, and survive submersion in water. We characterize critical mechanisms in textile-integrated soft circuits, including how textiles impact electromechanical performance of stretchable conductors, which informs how these techniques can be employed for wearable electronics across a range of applications. The use of multiple adhesion techniques enables our circuit construction, as both heat press processing and solvent welding are employed together to achieve strong interlayer adhesion within textile-integrated LM soft circuits. Using both techniques grants the ability to create multilayer circuits in our scheme without limiting the adhesion either to textiles or between circuit layers, ensuring the entire multilayer circuit has a robust construction. The structure–mechanics–functionality relationship we characterize for this layup allows for multilayer circuit designs to enable increases in functionality without significant penalties to deformability. For manipulations expected of wearable electronics, these textile-integrated circuits are shown to maintain electrical continuity under both extension and folding, as LM can deform and flow along with multiaxial mechanical strains. This provides a reliable inter-



connect between circuit elements for wearable electronics, including resistances low enough to enable longer transmission distances. Environmental resilience is also shown through submersion in water, demonstrating the inherent ruggedness of these soft circuits and their benefits for underwater wearables.

With this method, wearable electronics can be made to suit many different complex applications, such as our wearable bird's eye view imaging system. Multilayer construction enables the manufacture of complex soft circuits, as does the integration of many types of rigid components; many electronic functionalities are not possible with the single-layer-only designs present in many prior works on LM soft circuits. As improving circuit complexity is currently a primary challenge in the LM field, advancement into multilayer LM circuits and manufacturing methods is crucial. Additionally, the fabrication method uses techniques such as lamination and spray deposition that could be integrated into high-speed, roll-to-roll manufacturing processes in future work. By using the adhesion of multiple elastomer layers and the extensibility and conformability of LM wires to create stretchable soft circuits which are robustly integrated with textiles, a new scheme for wearable electronics is achieved with both ruggedness for various environments and multilayer construction for advanced wearable devices.

Experimental

LM fabrication

Eutectic gallium-indium (EGaIn) liquid metal was made by combining a 3:1 by mass ratio of gallium and indium on a hot plate at 200°C overnight.



SIS sheet fabrication

A 1:5 by mass mixture of 35 g SIS pellets (Sigma-Aldrich part 432393) and 175 g toluene was combined in a 250 mL airtight jar and kept on a hot plate at 55 °C with a stir bar until fully dissolved. SIS sheets were made by casting 10 g of SIS:toluene mixture into a 110 mm by 85 mm laser cut acrylic (McMaster part 8589K42) mold coated in mold release (Ease Release 200). These were left for 24 hours in a fume hood such that the toluene evaporates, and the SIS sheets which remain were removed and demolded by hand. Edges were trimmed to remove any meniscus that formed at the edge of the mold. The thickness of the final SIS sheet is 0.20 – 0.25 mm.

Heat press processing for SIS and textile adhesion

SIS sheets used in adhesion tests were adhered to textiles using a heated press (Carver Bench Top Model 4120) at 200 °C and 500 kPa for 3 minutes. To achieve a smoother surface for use in demonstration samples utilizing LM, some samples were prepared at only 150 °C. The processing parameters for hot melt adhesion were determined through an investigation using Box-Behnken methods on several textiles; results were generalized to the full selection of textiles using a scoring system (Fig. S12).

Textile-integrated LM soft circuit fabrication

SIS sheets for each layer were cut to desired size with holes for *vias* and rigid components using a laser cutter (Universal Laser Systems VLS4.75). Spray masks (Blazer Orange Laser Mask, Johnson Plastics Plus) were cut to the desired trace pattern for each layer. LM was spray-coated with an airbrush onto the first layer (SIS sheet heat pressed to textile) using a mask. Toluene is applied to the surface using a misting spray bottle, and the next SIS layer is placed on top in alignment with the circuit pattern. Toluene is evaporated by leaving the circuit in a fume hood overnight. LM is spray-coated onto the second layer with the proper



mask for its desired pattern. This process is repeated for any subsequent layers as desired.

Once all layers are made, rigid components are placed and the circuit is encapsulated by either solvent welding another SIS film or casting additional SIS:toluene mixture on top.

Adhesive peel testing

Adhesion was measured using T-peel geometry based on ASTM D1876 on an Instron 5944 Universal Testing Machine. Samples were prepared in panels 75 mm wide by 175 mm long, bonded over 100 mm of their length. Three test specimens were cut from each panel to a width of 25 mm. Adhesive fracture energy was calculated using $G_c = 2F_c/w$, where F_c is the critical force in the steady-state plateau region of the load-displacement curve during peel (See inset of Fig. 2a).

Tensile electromechanical testing

Sheets of SIS and SIS bonded to polyester spandex (Fabric Wholesale Direct SKU SV578475) were cut into tensile dog bone specimens of 50% size of the ASTM D412 type C standard using a die cutter. Copper tape was applied the ends of a specimen, and LM was deposited as a single soft wire using a spray mask and airbrush. Another SIS dog bone specimen was applied via solvent welding with toluene to encapsulate the LM soft wire. Specimens were tested using a Instron 5944 Universal Testing Machine at a rate of 60 mm/min until mechanical fracture, and the electrical resistance was simultaneously measured by a Keithley 2461 SourceMeter connected to the copper tape interfaces at each end of the LM soft wire.

Cyclic folding electromechanical testing

Sheets of SIS and SIS bonded to polyester spandex (Fabric Wholesale Direct SC578446) and 600D Polyester (Rockywoods RBC600) were cut into rectangles of 10 x 100 mm using a laser cutter. Copper tape was applied the ends of a specimen, and LM was deposited as



a single soft wire using a spray mask and airbrush. Another layer of SIS was applied via solvent welding with toluene to encapsulate the LM soft wire. Specimens were tested using a custom setup consisting of a position control motor (DYNAMIXEL XC430-T150BB-T) and 3D-printed grips (Bambu Lab P1S and Verbatim #55000 ABS filament), which rotates across a 270° arc (Supplementary video S2). The electrical resistance was simultaneously measured by a Keithley 2461 SourceMeter connected to the copper tape interfaces at each end of the LM soft wire.

Water immersion test

A sample circuit with a CR1220 coin cell battery (Digikey part numbers SY033-ND and 36-1056-ND), LED, and resistor (Digikey part number A116039CT-ND) was prepared. A 4 ft long by 3 in diameter plastic tube (McMaster part number 9176T17) was sealed at one end and filled with tap water. The circuit was attached to a weighted line and inserted into the water-filled tube such that it was at a depth of 1 m, while being observed by a camera for continuous operation of the LED for 30 minutes.

Wearable sensing headband fabrication

The wearable sensing headband circuit was fabricated in a flat configuration on a polyester spandex substrate using the methods previously described. During fabrication, copper tape was placed at the terminus of each LM soft wire, and a mixture of 5 volume percent copper powder (US Research Nanomaterials stock # US5002) in LM was applied in a small amount at the soft-rigid interface. In addition, the circuit was annealed in a 80 °C oven for approximately 72 hours after assembly to relieve residual stresses. Cameras (Weivision 360° Surround View System, Amazon part number B00ZR65O2G) were affixed to mounting brackets fabricated through 3D printing that clamp onto the headband, and their connection wires were soldered to the copper tape. An additional sheet of SIS was applied through solvent welding to connect the two ends of the circuit, forming the headband shape. The



wearable circuit is connected to a mini-computer which computes the stitched overhead view. This system is powered by a battery (Turnigy 12000 mAh 4S LiPo pack, HobbyKing SKU 9067000425-0).

Author Contributions

B.T.W. and M.D.B. conceived the idea; B.T.W. and E.T.W. designed systems and components with input from M.D.B; B.T.W. and E.T.W. fabricated components and performed experiments; B.T.W. and E.T.W. analyzed data; B.T.W., E.T.W. and M.D.B. wrote the paper; and M.D.B. supervised the study.

Conflicts of Interest

The authors declare no competing interests.

Data Availability Statement

Data available on request from the authors.

Acknowledgments

We acknowledge support from the Office of Naval Research Young Investigator Program (YIP) (N000142112699).

References

- [1] Soon Wan Chung and Hyun Tae Kim. Interfacial reliability between hot-melt polyamides resin and textile for wearable electronics application. *Microelectronics Reliability*,



52(7):1501–1510, jul 2012.

- [2] Séverine de Mulatier, Mohamed Nasreldin, Roger Delattre, Marc Ramuz, and Thierry Djenizian. Electronic Circuits Integration in Textiles for Data Processing in Wearable Technologies. *Advanced Materials Technologies*, 3(10):1700320, oct 2018.
- [3] Malte von Krshiwoblozki, Torsten Linz, Andreas Neudeck, and Christine Kallmayer. Electronics in Textiles – Adhesive Bonding Technology for Reliably Embedding Electronic Modules into Textile Circuits. In *Wearable/Wireless Body Sensor Networks for Healthcare Applications*, volume 85, pages 1–10, sep 2012.
- [4] Eunah Heo, Keun Yeong Choi, Jooyong Kim, Jong Hu Park, and Hojin Lee. A wearable textile antenna for wireless power transfer by magnetic resonance. *Textile Research Journal*, 88(8):913–921, apr 2018.
- [5] Han-Joon Kim, Rongzhou Lin, Sippanat Achavananthadith, and John S. Ho. Near-field-enabled Clothing for Wearable Wireless Power Transfer. In *2020 IEEE Wireless Power Transfer Conference (WPTC)*, pages 22–25. IEEE, nov 2020.
- [6] Teppei Araki, Masaya Nogi, Katsuaki Suganuma, Masaro Kogure, and Osamu Kirihara. Printable and Stretchable Conductive Wirings Comprising Silver Flakes and Elastomers. *IEEE Electron Device Letters*, 32(10):1424–1426, oct 2011.
- [7] Braden M. Li, Ozkan Yildiz, Amanda C. Mills, Tashana J. Flewwellin, Philip D. Bradford, and Jesse S. Jur. Iron-on carbon nanotube (CNT) thin films for biosensing E-Textile applications. *Carbon*, 168:673–683, oct 2020.
- [8] Konstantin Klamka, Raimund Dachzelt, and Jürgen Steimle. Rapid iron-on user interfaces: Hands-on fabrication of interactive textile prototypes. In *Proceedings of the 2020 CHI Conference on Human Factors in Computing Systems*, volume 20, pages 1–14. ACM, 4 2020. This is the same as another, need to remove one.



- [9] Thomas Vervust, Frederick Bossuyt, Fabrice Axisa, and Jan Vanfleteren. Stretchable and Washable Electronics for Embedding in Textiles. *MRS Proceedings*, 1271:1271–JJ04–03, feb 2010.
- [10] Eric J Markvicka, Michael D Bartlett, Xiaonan Huang, and Carmel Majidi. An autonomously electrically self-healing liquid metal–elastomer composite for robust soft-matter robotics and electronics. *Nature materials*, 17(7):618–624, 2018.
- [11] Ravi Tutika, A. B. M. Tahidul Haque, and Michael D. Bartlett. Self-healing liquid metal composite for reconfigurable and recyclable soft electronics. *Communications Materials*, 2(1):1–8, 2021.
- [12] Wuzhou Zu, Yunsik Ohm, Manuel Reis Carneiro, Michael Vinciguerra, Mahmoud Tavakoli, and Carmel Majidi. A Comparative Study of Silver Microflakes in Digitally Printable Liquid Metal Embedded Elastomer Inks for Stretchable Electronics. *Advanced Materials Technologies*, 7(12):2200534, dec 2022.
- [13] Yanyan Li, Shuxuan Feng, Shitai Cao, Jiaxue Zhang, and Desheng Kong. Printable Liquid Metal Microparticle Ink for Ultrastretchable Electronics. *ACS Applied Materials Interfaces*, 12(45):50852–50859, nov 2020.
- [14] Liqing Ai, Weikang Lin, Limei Ai, Yannan Li, Mengyi Qiang, Xiaoya Wang, Min Shi, Zhengbao Yang, and Xi Yao. “heat-press-n-go” stretchable interconnects enabled by liquid metal conductor with supramolecular confinement. *Advanced Functional Materials*, n/a(n/a):2425264, 2025.
- [15] Tyler A. Pozarycki, Dohgyu Hwang, Edward J. Barron, Brittan T. Wilcox, Ravi Tutika, and Michael D. Bartlett. Tough Bonding of Liquid Metal-Elastomer Composites for Multifunctional Adhesives. *Small*, 18(41):1–9, 2022.
- [16] Simok Lee, Syed Ahmed Jaseem, Nurit Atar, Meixiang Wang, Jeong Yong Kim, Mohammadreza Zare, Sooyoung Kim, Michael D Bartlett, Jae-Woong Jeong, and Michael D



- Dickey. Connecting the dots: Sintering of liquid metal particles for soft and stretchable conductors. *Chemical Reviews*, 125(6):3551–3585, 2025.
- [17] Ethan B Secor, Alexander B Cook, Christopher E Tabor, Mark C Hersam, E B Secor, M C Hersam, A B Cook, and C E Tabor. Wiring up Liquid Metal: Stable and Robust Electrical Contacts Enabled by Printable Graphene Inks. *Advanced Electronic Materials*, 4(1):1700483, jan 2018.
- [18] A B M Tahidul Haque, Ravi Tutika, Meng Gao, Angel Martinez, Julie Mills, J. Arul Clement, Junfeng Gao, Mohsen Tabrizi, M. Ravi Shankar, Qibing Pei, and Michael D Bartlett. Conductive liquid metal elastomer thin films with multifunctional electro-mechanical properties. *Multifunctional Materials*, 3(4):044001, dec 2020.
- [19] A. B.M.Tahidul Haque, Dong Hae Ho, Dohgyu Hwang, Ravi Tutika, Chanhong Lee, and Michael D. Bartlett. Electrically Conductive Liquid Metal Composite Adhesives for Reversible Bonding of Soft Electronics. *Advanced Functional Materials*, 2304101:1–10, 2023.
- [20] Tyler A. Pozarycki, Wuzhou Zu, Brittan T. Wilcox, and Michael D. Bartlett. A Flexible and Electrically Conductive Liquid Metal Adhesive for Hybrid Electronic Integration. *Advanced Functional Materials*, 2313567:1–9, 2024.
- [21] Suji Choi, Jinkyung Park, Wonji Hyun, Jangwon Kim, Jaemin Kim, Young Bum Lee, Changyeong Song, Hye Jin Hwang, Ji Hoon Kim, Taeghwan Hyeon, and Dae Hyeong Kim. Stretchable Heater Using Ligand-Exchanged Silver Nanowire Nanocomposite for Wearable Articular Thermotherapy. *ACS Nano*, 9(6):6626–6633, jun 2015.
- [22] Helapiyumi Weerathunga, Thu Trang Do, Hong Duc Pham, Robert Jones, Jennifer Macleod, Taeyoung Kim, and Deepak Dubal. Washable and Flexible All Carbon Electrothermal Joule Heater for Electric Vehicles. 2023.



- [23] Yu Song, Jihong Min, You Yu, Haobin Wang, Yiran Yang, Haixia Zhang, and Wei Gao. Wireless battery-free wearable sweat sensor powered by human motion. *Science Advances*, 6(40):9842, oct 2020.
- [24] Harish Chander, Reuben F. Burch, Purva Talegaonkar, David Saucier, Tony Luczak, John E. Ball, Alana Turner, Sachini N.K. Kodithuwakku Arachchige, Will Carroll, Brian K. Smith, Adam Knight, and Raj K. Prabhu. Wearable stretch sensors for human movement monitoring and fall detection in ergonomics, may 2020.
- [25] Eric J Markvicka, Ravi Tutika, Michael D Bartlett, and Carmel Majidi. Soft electronic skin for multi-site damage detection and localization. *Advanced Functional Materials*, 29(29):1900160, 2019.
- [26] Mohammed G Mohammed and Rebecca Kramer. All-printed flexible and stretchable electronics. *Advanced Materials*, 29(19):1604965, 2017.
- [27] Austin Lancaster and Manish Keswani. Integrated circuit packaging review with an emphasis on 3d packaging. *Integration*, 60:204–212, 2018.
- [28] Stephanie J. Woodman, Dylan S. Shah, Melanie Landesberg, Anjali Agrawala, and Rebecca Kramer-Bottiglio. Stretchable arduinos embedded in soft robots. *Science Robotics*, 9(94):eadn6844, 2024.
- [29] Shanliangzi Liu, Dylan S Shah, and Rebecca Kramer-Bottiglio. Highly stretchable multi-layer electronic circuits using biphasic gallium-indium. *Nature Materials*, 20(6):851–858, 2021.
- [30] Pedro Alhais Lopes, Daniel Félix Fernandes, André F. Silva, Daniel Green Marques, Aníbal T. De Almeida, Carmel Majidi, and Mahmoud Tavakoli. Bi-Phasic Ag-In-Ga-Embedded Elastomer Inks for Digitally Printed, Ultra-Stretchable, Multi-layer Electronics. *ACS Applied Materials and Interfaces*, 13(12):14552–14561, mar 2021.



- [31] Chengjun Zhang, Qing Yang, Haoyu Li, Zexiang Luo, Yu Lu, Jialiang Zhang, Cheng Li, and Feng Chen. 3d laser structuring of supermetalphobic microstructures inside elastomer for multilayer high-density interconnect soft electronics. *International Journal of Extreme Manufacturing*, 7(3):035004, 2025.
- [32] Jangyeol Yoon, Soo Yeong Hong, Yein Lim, Seung-Jung Lee, Goangseup Zi, and Jeong Sook Ha. Design and fabrication of novel stretchable device arrays on a deformable polymer substrate with embedded liquid-metal interconnections. *Advanced Materials (Deerfield Beach, Fla.)*, 26(38):6580–6586, 2014.
- [33] Dong Hae Ho, Chenhao Hu, Ling Li, and Michael D Bartlett. Soft electronic vias and interconnects through rapid three-dimensional assembly of liquid metal microdroplets. *Nature Electronics*, 7(11):1015–1024, 2024.
- [34] Mahmoud Tavakoli, Pedro Alhais Lopes, Abdollah Hajalilou, André F Silva, Manuel Reis Carneiro, José Carvalheiro, João Marques Pereira, and Aníbal T. de Almeida. 3R Electronics: Scalable Fabrication of Resilient, Repairable, and Recyclable Soft-Matter Electronics. *Advanced Materials*, 34(31):2203266, aug 2022.
- [35] Abdollah Hajalilou, Elahe Parvini, Tiago A. Morgado, Pedro Alhais Lopes, M. Estrela Melo Jorge, Marta Freitas, and Mahmoud Tavakoli. Replacing the gallium oxide shell with conductive ag: Toward a printable and recyclable composite for highly stretchable electronics, electromagnetic shielding, and thermal interfaces. *ACS Applied Materials & Interfaces*, 0(0):null, 0. PMID: 39469861.
- [36] Yidong Peng, Jiancheng Dong, Jiahui Sun, Yanheng Mao, Yuxi Zhang, Jiayan Long, Le Li, Chao Zhang, Yan Zhao, Hengyi Lu, Hai-Long Qian, Xiu-Ping Yan, Jianhua Zhao, Fangneng Wang, Yunpeng Huang, and Tianxi Liu. Multimodal health monitoring via a hierarchical and ultrastretchable all-in-one electronic textile. *Nano Energy*, 110:108374, 2023.



- [37] Jiayi Yang, Praneshnandan Nithyanandam, Shreyas Kanetkar, Ki Yoon Kwon, Jinwoo Ma, Sooik Im, Ji-Hyun Oh, Mohammad Shamsi, Mike Wilkins, Michael Daniele, Tae-il Kim, Huu Ngoc Nguyen, Vi Khanh Truong, and Michael D. Dickey. Liquid metal coated textiles with autonomous electrical healing and antibacterial properties. *Advanced Materials Technologies*, 8(14):2202183, 2023.
- [38] Chunyan Cao, Hang Su, Liqing Ai, Dong Lv, Jing Gu, Ruiqing Li, Dawei Li, Wei Zhang, Mingzheng Ge, and Xi Yao. Highly stable liquid metal-based electronic textiles by adaptive interfacial interactions. *Advanced Functional Materials*, 34(49):2409586, 2024.
- [39] Rachel A. Shveda, Anoop Rajappan, Te Faye Yap, Zhen Liu, Marquise D. Bell, Barclay Jumet, Vanessa Sanchez, and Daniel J. Preston. A wearable textile-based pneumatic energy harvesting system for assistive robotics. *Science Advances*, 8(34):eabo2418, 2022.
- [40] Barclay Jumet, Zane A. Zook, Anas Yousaf, Anoop Rajappan, Doris Xu, Te Faye Yap, Nathaniel Fino, Zhen Liu, Marcia K. O'Malley, and Daniel J. Preston. Fluidically programmed wearable haptic textiles. *Device*, 1(3):100059, 2023.
- [41] Jinsil Kim, Jiabin Fan, Gayaneh Petrossian, Xin Zhou, Pierre Kateb, Noemy Gagnon-Lafrenais, and Fabio Cicoira. Self-healing, stretchable and recyclable polyurethane-pedot:pss conductive blends. *Mater. Horiz.*, 11:3548–3560, 2024.
- [42] Rumin Liu, Kequan Xia, Tao Yu, Feng Gao, Qinghua Zhang, Liping Zhu, Zhizhen Ye, Shikuan Yang, Yaoguang Ma, and Jianguo Lu. Multifunctional smart fabrics with integration of self-cleaning, energy harvesting, and thermal management properties. *ACS nano*, 18(45):31085–31097, 2024.
- [43] Zhenyun Zhao, Kequan Xia, Yang Hou, Qinghua Zhang, Zhizhen Ye, and Jianguo Lu. Designing flexible, smart and self-sustainable supercapacitors for portable/wearable



- electronics: from conductive polymers. *Chemical Society Reviews*, 50(22):12702–12743, 2021.
- [44] Yun Liang, Peng Xiao, Feng Ni, Ling Zhang, Tao Zhang, Shuai Wang, Wei Zhou, Wei Lu, Shiao-Wei Kuo, and Tao Chen. Biomimetic underwater self-perceptive actuating soft system based on highly compliant, morphable and conductive sandwiched thin films. *Nano Energy*, 81:105617, mar 2021.
- [45] Xiangjun Qi, Hongtao Zhao, Lihong Wang, Fengqiang Sun, Xiaorui Ye, Xueji Zhang, Mingwei Tian, and Lijun Qu. Underwater sensing and warming E-textiles with reversible liquid metal electronics. *Chemical Engineering Journal*, 437:135382, jun 2022.
- [46] Hamed Pourkheyrollah, Peyman Fayyaz Shahandashti, Ali Meimandi, Amir Jahanshahi, and Hassan Ghafoorifard. On Economically Viable Stretchable Washable Electronics Technology: Proof of Concept. In *2019 27th Iranian Conference on Electrical Engineering (ICEE)*, pages 285–289. IEEE, apr 2019.
- [47] Jonathan T. Reeder, Jungil Choi, Yeguang Xue, Philipp Gutruf, Justin Hanson, Mark Liu, Tyler Ray, Amay J. Bandodkar, Raudel Avila, Wei Xia, Siddharth Krishnan, Shuai Xu, Kelly Barnes, Matthew Pahnke, Roozbeh Ghaffari, Yonggang Huang, and John A. Rogers. Waterproof, electronics-enabled, epidermal microfluidic devices for sweat collection, biomarker analysis, and thermography in aquatic settings. *Science Advances*, 5(1), jan 2019.
- [48] Shao-Hao Lu, Yi Li, and Xueju Wang. Soft, flexible conductivity sensors for ocean salinity monitoring. *J. Mater. Chem. B*, 11:7334–7343, 2023.
- [49] Yi Li, Guangfu Wu, Gyuhong Song, Shao Hao Lu, Zizheng Wang, He Sun, Yi Zhang, and Xueju Wang. Soft, pressure-tolerant, flexible electronic sensors for sensing under harsh environments. *ACS Sensors*, 7:2400–2409, 8 2022.



- [50] Shaoyu Liu, Daohui Zhang, Xin Fu, Liyan Mo, Qile Miao, Rong Huang, Xin Huang, Wei Guo, Yangyang Li, Qingyang Zheng, Ganguang Yang, Kun Bai, Bin Xie, Zhoupin Yin, and Hao Wu. Tactile sensing for soft robotic manipulators in 50mpa hydrostatic pressure environments. *Advanced Intelligent Systems*, 5:2300296, 12 2023.
- [51] Edward J. Barron, Ella T. Williams, Brittan T. Wilcox, Dong Hae Ho, and Michael D. Bartlett. Liquid metal-elastomer composites for water-resilient soft electronics. *Journal of Polymer Science*, (September):1–12, nov 2023.
- [52] Chi-hyeong Kim, Jinsil Kim, Jiabin Fan, Meijing Wang, and Fabio Cicoira. Recyclable printed liquid metal composite for underwater stretchable electronics. *Small Science*, page 2400553, 2025.
- [53] Insang You, Minsik Kong, and Unyong Jeong. Block Copolymer Elastomers for Stretchable Electronics. *Accounts of Chemical Research*, 52(1):63–72, jan 2019.
- [54] Costantino Creton, Guangjun Hu, Fanny Deplace, Leslie Morgret, and Kenneth R. Shull. Large-strain mechanical behavior of model block copolymer adhesives. *Macromolecules*, 42(20):7605–7615, oct 2009.
- [55] Dae Jun Kim, Hyun Joong Kim, and Goan Hee Yoon. Effects of blending and coating methods on the performance of SIS (styrene-isoprene-styrene)-based pressure-sensitive adhesives. *Journal of Adhesion Science and Technology*, 18(15-16):1783–1797, 2004.
- [56] Dae Jun Kim, Hyun Joong Kim, and Goan Hee Yoon. Shear creep resistance of styrene-isoprene-styrene (SIS)-based hot-melt pressure-sensitive adhesives. *Journal of Applied Polymer Science*, 100(1):825–831, apr 2006.
- [57] Dae Jun Kim, Wyun Joong Kim, and Goan Hee Yoon. Tack and fracture energy of tackified SIS (styrene-isoprene-styrene)-based hot-melt pressure sensitive adhesives (HMPSAs). *Journal of Adhesion Science and Technology*, 20(12):1367–1381, 2006.



- [58] F. X. Gibert, G. Marin, C. Derail, A. Allal, and J. Lechat. Rheological properties of hot melt pressure-sensitive adhesives based on styrene - Isoprene copolymers. Part 1: A rheological model for [SIS-SI] formulations. *Journal of Adhesion*, 79(8-9):825–852, aug 2003.
- [59] Jing Xue, Jing Wang, Haofer Huang, Ming Wang, Yali Zhang, and Lijuan Zhang. Feasibility of processing hot-melt pressure-sensitive adhesive (Hmpsa) with solvent in the lab. *Processes*, 9(9):1608, sep 2021.
- [60] J.M. Widmaier and G.C. Meyer. Molecular-Weight Dependence of the Glass Transition Temperatures of Rigid SIS Triblock Copolymers Studied by DSC. *Journal of Thermal Analysis*, 23:193–199, 1982.
- [61] Michael D Bartlett, Scott W Case, Anthony J Kinloch, and David A Dillard. Peel tests for quantifying adhesion and toughness: A review. *Progress in Materials Science*, 137:101086, 2023.
- [62] Dinara Zhalmuratova, Thanh Giang La, Katherine Ting Ting Yu, Alexander R.A. Szojka, Stephen H.J. Andrews, Adetola B. Adesida, Chun Il Kim, David S. Nobes, Darren H. Freed, and Hyun Joong Chung. Mimicking "j-Shaped" and Anisotropic Stress-Strain Behavior of Human and Porcine Aorta by Fabric-Reinforced Elastomer Composites. *ACS Applied Materials and Interfaces*, 11(36):33323–33335, sep 2019.
- [63] Xiaoyao Xu, Guowen Wang, Han Yan, and Xuefeng Yao. Constitutive relationship of fabric rubber composites and its application, jan 2023.
- [64] Dinara Zhalmuratova and Hyun Joong Chung. Reinforced Gels and Elastomers for Biomedical and Soft Robotics Applications. *ACS Applied Polymer Materials*, 2(3):1073–1091, mar 2020.
- [65] Pradeep Lall, Hyesoo Jang, Ben Leever, and Scott Miller. Folding-Reliability of Flexible Electronics in Wearable Applications. *ASME 2019 International Technical Conference*



and Exhibition on Packaging and Integration of Electronic and Photonic Microsystems, InterPACK 2019, dec 2019.

- [66] Thomas Chalklen, Michael Smith, and Sohini Kar-Narayan. Improved fatigue resistance in transfer-printed flexible circuits embedded in polymer substrates with low melting temperatures. *Flexible and Printed Electronics*, 8(2):025014, may 2023.
- [67] Seol-Min Yi, In-Suk Choi, Byoung-Joon Kim, and Young-Chang Joo. Reliability Issues and Solutions in Flexible Electronics Under Mechanical Fatigue. *Electronic Materials Letters*, 14(4):387–404, jul 2018.
- [68] Ho-Young Lee, Seol-Min Yi, Ji-Hoon Lee, Hwan-Soo Lee, Seungmin Hyun, and Young-Chang Joo. Effects of bending fatigue on the electrical resistance in metallic films on flexible substrates. *Metals and Materials International*, 16(6):947–951, dec 2010.
- [69] Byoung-Joon Kim, Myeong-Hyeok Jeong, Hwang Sung-Hwan, Ho-Young Lee, Sung-Won Lee, Ki-Do Chun, Young-Bae Park, and Young-Chang Joo. Relationship between tensile characteristics and fatigue failure by folding or bending in cu foil on flexible substrate. *Journal of the Microelectronics Packaging Society*, 18:55–59, 2011.
- [70] F. Bossuyt, J. Guenther, T. Löher, M. Seckel, T. Sterken, and J. de Vries. Cyclic endurance reliability of stretchable electronic substrates. *Microelectronics Reliability*, 51(3):628–635, mar 2011.
- [71] Andrea Karen Persons, John E. Ball, Charles Freeman, David M. Macias, Chartrisa Lashan Simpson, Brian K. Smith, and Reuben V.F. Burch. Fatigue testing of wearable sensing technologies: Issues and opportunities. *Materials*, 14(15):4070, aug 2021.
- [72] Guorui Li, Xiangping Chen, Fanghao Zhou, Yiming Liang, Youhua Xiao, Xunuo Cao, Zhen Zhang, Mingqi Zhang, Baosheng Wu, Shunyu Yin, et al. Self-powered soft robot in the mariana trench. *Nature*, 591(7848):66–71, 2021.



Data Availability Statement

Data available on request from the authors.

Open Access Article. Published on 25 2025. Downloaded on 29.07.2025 18:24:04.
This article is licensed under a Creative Commons Attribution 3.0 Unported Licence.

